Electronic Supplementary Information (ESI)

Efficient Solar Photoelectrolysis by Nanoporous Mo:$BiVO_4$ Through Controlled Electron Transport

*Jason A. Seabold, Kai Zhu and Nathan R. Neale**

Chemical and Materials Science Center, National Renewable Energy Laboratory, Golden, CO 80401, USA

General Details

300 nm, 1.8% Mo doped $BiVO_4$ films (1.8 cm^2 active area) on FTO were used for all tests. Each had an initial photocurrent density of *ca*. 3 mA/cm^2 at 1.23 V vs. RHE in 0.1 M Na_2SO_3, 0.1 M NaH_2PO_4 at pH 7 under 1 sun. Unless otherwise noted, photocurrent to test the catalysts was conducted using a 300 W Xe arc lamp (Newport) calibrated to 1 Sun and in a 0.1 M NaH_2PO_4 electrolyte at pH 7 under 1 sun intensity. A 3-electrode cell was employed, including a $BiVO_4$ working electrode, Pt foil counter electrode, and Ag/AgCl reference electrode. 1 M instead of 0.1 M NaH_2PO_4 was used in the main text when testing FeOOH films. This alleviates a slight ion diffusion limitation, providing a <10% enhancement. Thus, the 0.1 M buffer concentration cannot be the major factor used to explain the very poor performance of the following catalysts.

Catalyst Loadings

For the catalysts that were photodeposited, the photodeposition inherently indicates whether the catalyst film is too thick/resistive by a decrease of the photodeposition

current with time. Thus catalyst photodepositions were stopped at or before this point. For some photodepositions such as MnO_x and Cu-carbonate, the photodeposition current was so extremely poor from the initial stage of the photodeposition that it was obvious that even a very thin layer of catalyst was degrading the photocurrent, likely due to interfacial states that resulted in increased recombination rates. In cases where catalysts were soaked, dipped, or drop cast, different loadings were tested and all resulted in low photocurrent performance. The homogeneous carbonate catalyst is well documented to perform best under concentrated conditions, so 1 M concentration was used, which is the solubility limit of $NaHCO_3$.

Ag^+

$BiVO_4$ was soaked for 14 and 96 hours in a 10 mM $AgNO_3$ solution[1]. After rinsing in DI water, photocurrent in 0.1 M NaH_2PO_4 at pH 7 under 1 sun intensity gave < 1 mA/cm^2 at 1.23 V vs. RHE.

Pt

Pt was photodeposited on $BiVO_4$ from 10 mM H_2PtCl_6 in 10 vol. % methanol 90 vol. % water (~ 2.5 M MeOH)[2]. $BiVO_4$ films were illuminated under 1 sun for 0.5, 3, and 30 minutes with no electrode attached (open circuit condition). This allows the electrons to reduce the Pt (IV) to Pt metal, while the holes oxidize methanol. Photocurrents in phosphate were 1-2 mA/cm^2 at 1.23 V vs. RHE at all values of Pt loading.

RuO_x

RuO_x was photodeposited from 5 mM hexammineruthenium (III) chloride at 0.2 V vs. Ag/AgCl for 2 minutes and 4 minutes, and at 1.8 V vs. RHE for 3 minutes and 12 minutes under 1 sun illumination. No films achieved a photocurrent density > 1 mA/cm^2 at 1.23 V vs. RHE in pH 7 phosphate.

MnO_x

MnO_x was photodeposited from 20 mM manganese (II) chloride at 0.2 V vs. Ag/AgCl for 2 minutes under 1 sun illumination. No film achieved a photocurrent density > 1 mA/cm^2 at 1.23 V vs. RHE in pH 7 phosphate.

NiO_x

NiO_x was photodeposited from 0.1 mM $NiSO_4$ in 1 M $NaHCO_3$, 0.1 M NaH_2PO_4, pH 7 at 0.4 V vs. Ag/AgCl under 1 sun illumination. Photocurrent in carbonate/phosphate had previously been determined to be stable, so this electrolyte was used to prevent photocorrosion during the NiO_x photodeposition (if, for example, the Ni^{2+} became diffusion limited, oxidation of carbonate would limit the photocorrosion). Photodeposition current density rose gradually from an initial 1.1 mA/cm^2 to 1.5 mA/cm^2 over 10 minutes. Then the current began to decline, signifying that the catalyst coverage had reached an optimum level, and the deposition was promptly stopped. The front illumination photocurrent density of the film was < 1.7 mA/cm^2 at 1.23 V vs. RHE in pH 7 phosphate. This could be from blockage of the light, but this is at best only a minor effect, as there was no visible difference in film color after NiO_x deposition.

Co-Pi

Photodeposition and electrodeposition of a small amount of Co-Pi OEC using conditions similar to literature[3] enhanced the photocurrent density at 1.23 V vs. RHE initially to *ca*. 80 % of the level of sulfite, but showed a rapid decay. Very short deposition times of a few seconds gave these types of results. Depositing a greater amount of Co-Pi did not alleviate this issue, but only resulted in very low photocurrent.

$Ni_{0.9}Fe_{0.1}O_x$

A solution of 2 mM $Fe(NO_3)_3$ and 20 mM $Ni(NO_3)_3$ and 1 drop Triton X-100 was prepared in ethanol to make $Ni_{0.9}Fe_{0.1}O_x$, which has been identified as one of the best OER catalysts[4]. A $BiVO_4$ film was dipped in the Ni/Fe solution with a withdrawal rate of 1 mm/s and allowed to dry at room temperature. Then it was heated 2 minutes at 300 °C on a hot plate. The film was cooled, then dipped again, dried, then heated to 300 °C for 5 minutes. Photocurrent density was < 0.1 mA/cm^2 at 1.23 V vs. RHE in pH 7 phosphate.

$NiFe_2O_4$

Nanocrystals of $NiFe_2O_4$ have recently been reported as a good catalyst for the OER[5]. Nanocrystals of $NiFe_2O_4$ were synthesized by a hot injection method reported previously for other metal oxide nanocrystals[6]. All chemicals were transferred air free from a glove box and heated on a schlenk line. Briefly, 3 g trioctylamine was heated to 300 °C with 800 rpm stirring over 30 minutes. A solution of 3 g oleylamine, 0.6 mmol $Fe(acac)_3$ and 0.3 mmol $Ni(acac)_2$ was injected from a gas-tight syringe into the 300 °C trioctylamine. Upon injection, the solution turned dark and dropped to 230 °C. It was increased to 250

°C over 5 minutes and then held at 250 °C for 30 minutes. The dark brown solution was cooled naturally to ~ 60 °C, then 2 mL toluene was added and the solution transferred to a centrifuge tube. The nanocrystals were precipitated with 30 mL methanol and collected by centrifugation. This was repeated twice more, and the final solids were easily dissolved in ~ 10 mL of 9:1 hexane:octene solution. The product was not weighed, but appeared to be ~ 50 mg. TEM shows ~5 nm nanocrystals (**Fig. S13**). X-ray fluorescence spectroscopy (XRF) was performed on a dropcast film of the $NiFe_2O_4$ nanocrystals, and revealed a 1.00:1.94 Ni:Fe ratio. X-ray diffraction (XRD) confirmed the expected spinel structure. A $BiVO_4$ film was dipped in the nanocrystal solution and allowed to dry, then repeated two more times. The film was almost imperceptibly darker. Then several drops of nanocrystal solution were dispersed on the surface of a second film, which dried very evenly. The final film was slightly darker than the first film, but still very transparent. Both of the $BiVO_4/NiFe_2O_4$ films were annealed at 425 °C in air for 1 h with 2 h ramp up and natural cooling. Photocurrent densities of $BiVO_4$ with the thin and thick $NiFe_2O_4$ layers only reached 0.4 mA/cm^2 and 0.1 mA/cm^2, respectively, at 1.23 V vs. RHE in pH 7 phosphate.

Cu-carbonate

A new catalyst, which involves dilute Cu^{2+} in a carbonate electrolyte, has recently demonstrated promise for water oxidation[7]. A $BiVO_4$ photoanode was operated in a 5 mM $CuCl_2$, 0.75 M K_2CO_3, pH 11.8 (natural pH) electrolyte sweeping from 0.3 V to 1.23 V vs. RHE at 10 mV/s under 1 sun illumination. The photocurrent density of the electrode at 1.23 V vs. RHE in this solution only reached about 0.6 mA/cm^2.

Carbonate

$BiVO_4$ has shown enhanced O_2 evolution when operated in carbonate containing electrolytes[8]. It is hypothesized to be due to the creation of a peroxocarbonate radical, which dimerizes then decomposes to form O_2 and two carbonate ions. Experiments in 1 M $NaHCO_3$ at pH 9.2 and in 1 M $NaHCO_3$, 0.1 M NaH_2PO_4 at pH 7 resulted in photocurrent densities of 2.3 to 2.5 mA/cm^2 at 1.23 V vs. RHE. This is about 75 % of the level attained for sulfite oxidation, not as high as the 88 % attained by FeOOH. Also, the fill factor was very poor, with very low photocurrent densities at lower applied potentials.

ICP Results		V / Bi		Mo / (Mo+V)	
		Expected	Experimental	Expected	Experimental
$BiVO_4$	Not Treated	2.25	2.26	0.00	0.00
	KOH Treated	1.00	1.07	0.00	0.00
Mo:$BiVO_4$	Not Treated	2.25	2.23	0.012	0.011
	KOH Treated	0.972 – 1.00	1.09	0.00 – 0.028	0.018

Fig. S1 ICP results for $BiVO_4$ and Mo:$BiVO_4$ films before and after 0.5 M KOH soak. The ranges listed for the KOH treated Mo:$BiVO_4$ sample reflect the maximum and minimum possible Mo incorporation. The minimum estimate of zero could occur if the Mo did not substitute into the lattice and instead formed MoO_3. In this case, it would be soluble in KOH and would be entirely removed. Each data value in the table is the average of two ICP samples. Each ICP sample was prepared by scraping material from ten 1.8 cm^2, 750 nm thick films (from 4.5 mm/s dip coat).

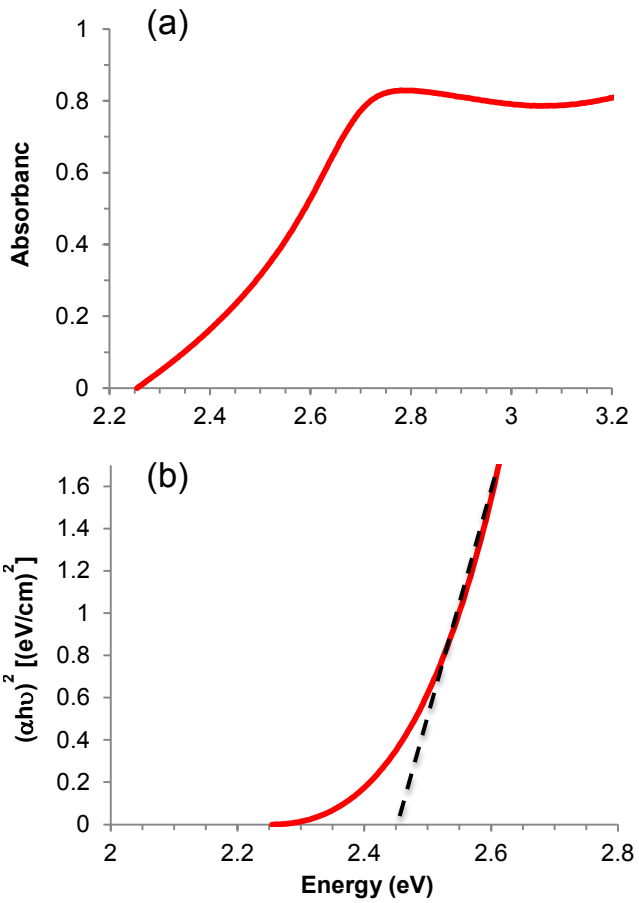

Fig. S2 Plots showing (a) absorption spectrum and (b) Tauc plot of a 750 nm $BiVO_4$ film on FTO, revealing a bandgap of 2.45 eV.

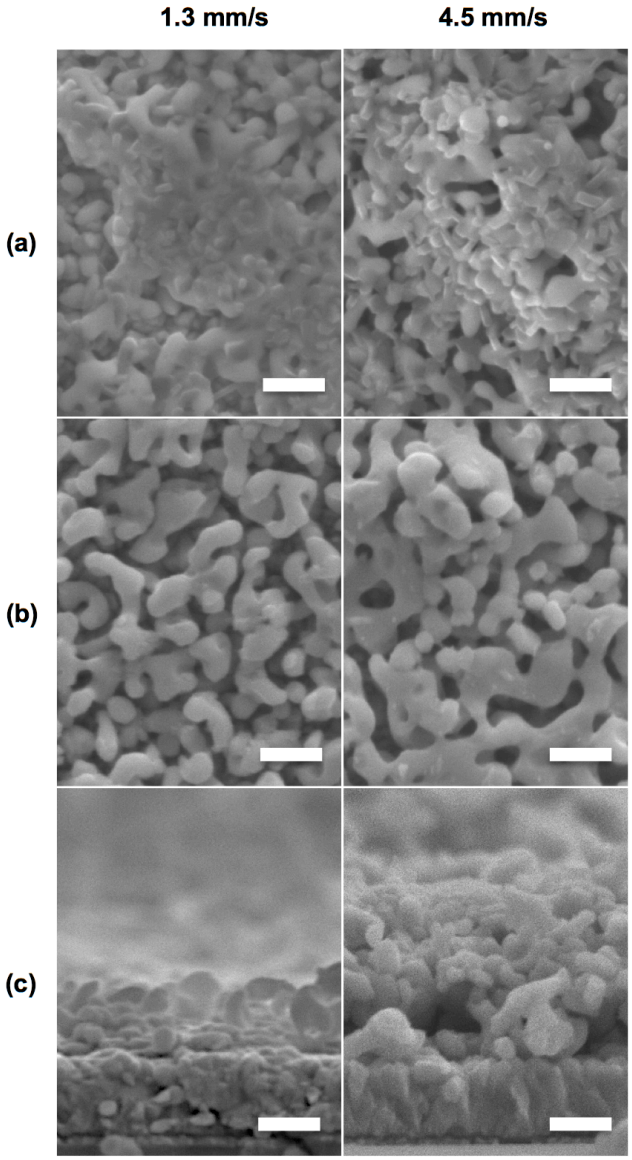

Fig. S3 SEM images of non-doped $BiVO_4$ films dipped at 1.3 mm/s (left column) and 4.5 mm/s (right column), showing top view (a) after annealing and (b) after annealing and KOH treatment and (c) cross-section after annealing and KOH treatment. The left column corresponds to 300 nm and the right column to 750 nm thick films. Scale bars are 250 nm.

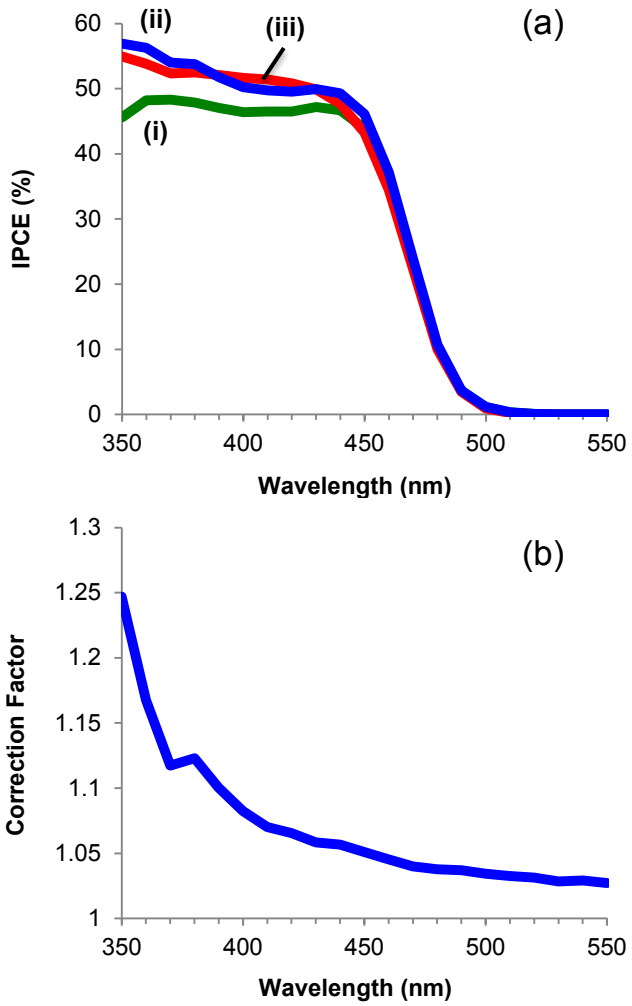

Fig. S4 (a) IPCE spectra of a 300 nm thick Mo:$BiVO_4$ film under (i) back illumination, (ii) back illumination with correction for FTO absorption, and (iii) front illumination. The data for front illumination and the data for back illumination after correction for FTO absorption match very well, confirming that the difference between front and back illumination is due to FTO absorption. (b) Plot of the correction factor at each wavelength derived from percent photons absorbed by FTO (% A_{FTO}) using the formula: correction factor = 100/(100 - % A_{FTO}). IPCE data collected under 1 sun illumination in 0.1 M Na_2SO_3, 0.1 M NaH_2PO_4, pH 7 electrolyte at 1.23 V vs. RHE. UV-vis data were collected with an integrating sphere as described in the experimental section of the main text.

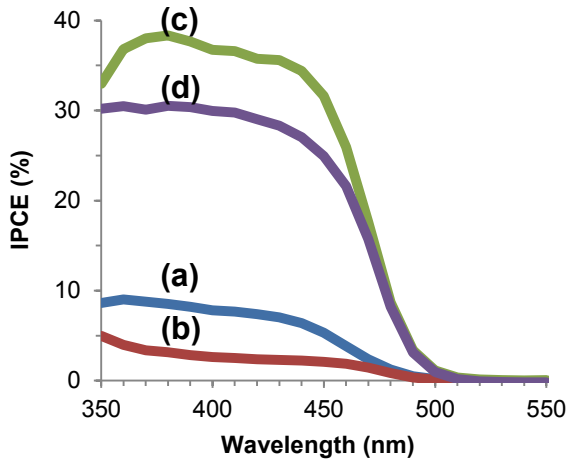

Fig. S5 IPCE spectra of a non-doped (a) back and (b) front illuminated $BiVO_4$ film, and Mo:$BiVO_4$ film with (c) back and (d) front illumination. Data collected in 0.1 M Na_2SO_3, 0.1 M NaH_2PO_4, pH 7 electrolyte at 1.23 V vs. RHE. Both films were 750 nm thick (4.5 mm/s dip coating rate).

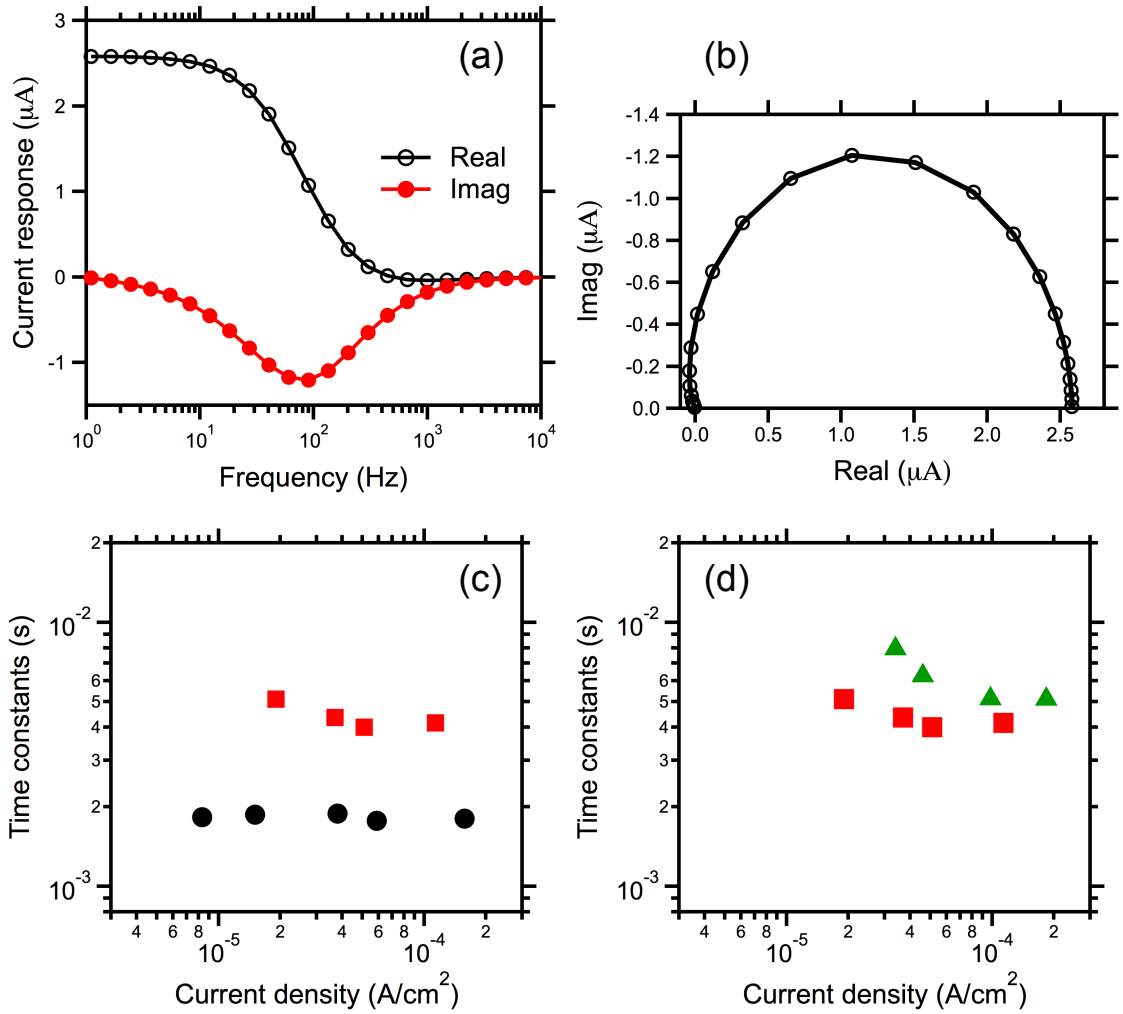

Fig. S6 Typical raw IMPS data are shown in (a) and (b) from a 300 nm Mo:$BiVO_4$ film. IMPS data display time constant versus photocurrent density to determine (c) the thickness dependence of back illuminated (■) 750 nm versus (●) 300 nm Mo:$BiVO_4$ and (d) the illumination direction dependence of (▲) front versus (■) back illuminated 750 nm Mo:$BiVO_4$ under varied intensities of a 455 nm LED. Data collected in 2-electrode cell with 0.1 M Na_2SO_3, 0.1 M NaH_2PO_4, pH 7 at 0.6 V vs. Pt counter electrode. All films were 1.8 % Mo doped.

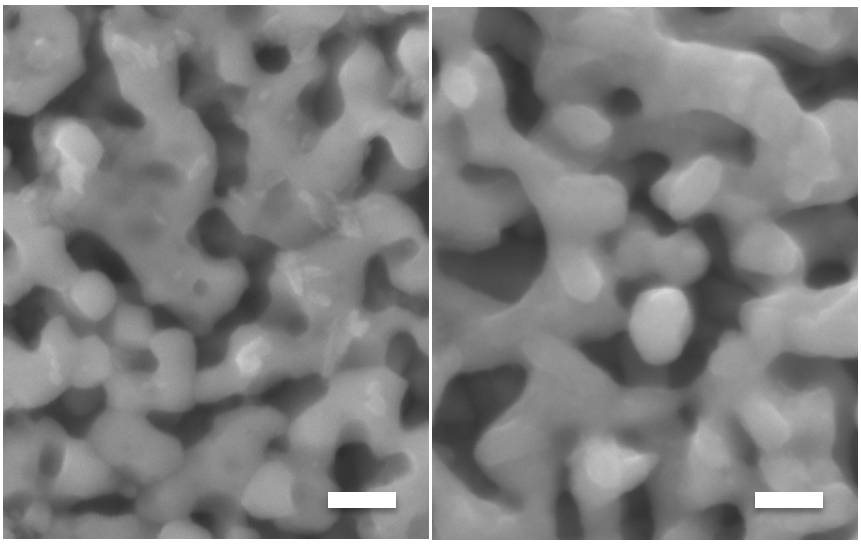

Fig. S7 SEM images of 300 nm Mo:$BiVO_4$ (a) bare and (b) with photodeposited FeOOH. No noticeable difference is seen, indicating that the FeOOH layer is very thin (<5 nm) and conformal. Scale bars are 100 nm.

Results	V / Bi			Fe / V			Fe / Bi		
	Expected	Experi-mental	Corrected	Expected	Experi-mental	Corrected	Expected	Experi-mental	Corrected
Bi-V-Fe standard	2.25	1.72	2.25	0.044	0.055	0.044	0.100	0.098	0.100
Mo:$BiVO_4$/ FeOOH KOH Treated	1.00	0.78	1.02	NA	0.111	0.086	NA	0.086	0.088

Fig. S8 EDX results for Mo:$BiVO_4$/FeOOH films. The standard was prepared as an annealed 300 nm sample without KOH treatment, and with an accurately known amount of $FeCl_2$ added to the precursor solution. Powder was scraped onto carbon tape supported on a Ni SEM stub. Data was corrected by a scale factor which was determined using the known ratio of elements in the standard. Each data point is the average of two separately prepared standards. The sample for analysis was prepared by scraping material from a 300 nm Mo:$BiVO_4$/FeOOH film (1.3 mm/s dip coating rate). Mo was not quantified, as 1.8% is near the limit of the detector. A calculation was performed to determine the required thickness of an FeOOH shell on a 75 nm $BiVO_4$ sphere to reach the observed 0.088 atomic Fe/Bi ratio. Elemental densities of Fe and Bi in the two materials were appropriately considered in the calculation, as was the fact that interparticle necking makes 100% coverage of each 75 nm $BiVO_4$ particle with an FeOOH shell impossible. Even with only a fractional coverage near 0.2, the required FeOOH shell thickness was <5 nm. If the estimated degree of inter-particle connectedness is decreased, exposing a greater percent of the surface of each 75 nm $BiVO_4$ sphere, the required FeOOH shell thickness shifts towards ≤1 nm.

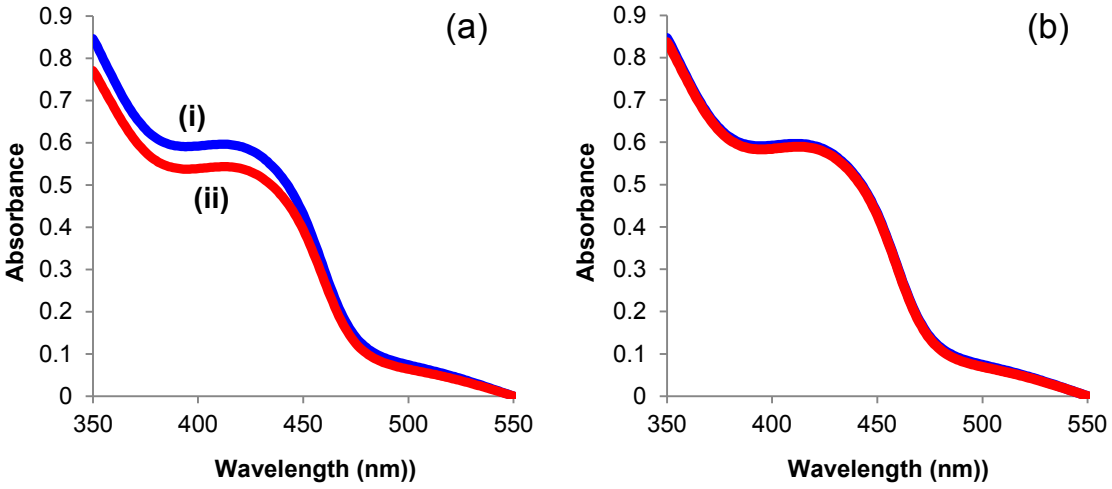

Fig. S9 Absorption profiles of a 300 nm Mo:$BiVO_4$ film on FTO before (i) and after (ii) FeOOH photodeposition. The films have slightly different profiles as seen in (a) likely due to random error such as slight differences in sample placement within the UV-vis. However, when normalized at 350 nm, they are overlaid precisely as seen in (b), suggesting that absorption from FeOOH has no effect on the observed photocurrent.

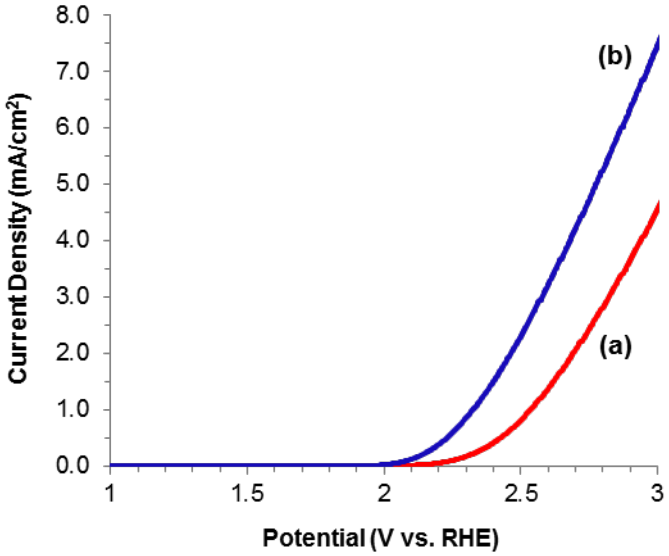

Fig. S10 Dark I-V curves of 300 nm thick films of (a) bare Mo:$BiVO_4$ and (b) Mo:$BiVO_4$/FeOOH. Potential was swept at 10 mV/s from 1 V to 3 V vs. RHE in 1 M NaH_2PO_4 at pH 7. The n-type $BiVO_4$ should act as a diode in reverse bias at high positive potentials, so no current should flow. The observed current implies that there is exposed FTO and possibly defects in the $BiVO_4$ that allow current to leak. FeOOH is present mainly on the $BiVO_4$ surface and not on the exposed FTO due to the selective nature of the photodeposition. Since the exposed FTO is likely the largest contributor to the catalytic current, the resulting difference between the dark catalytic currents of the $BiVO_4$ and $BiVO_4$/FeOOH will likely seem less than anticipated.

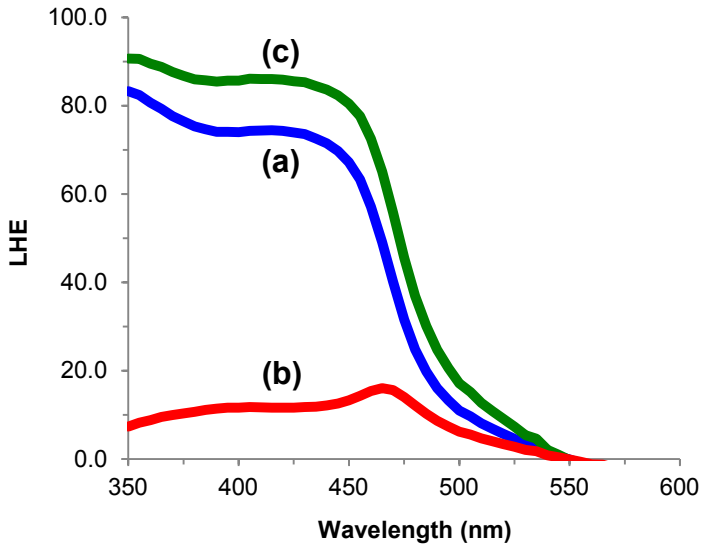

Fig. S11 Plot of light harvesting efficiency (a) measured for a single 300 nm Mo:$BiVO_4$ sample; and computed for (b) a theoretical identical rear electrode only receiving the transmitted light from the front electrode and (c) a theoretical double stack (sum of the experimental front electrode (a) and theoretical rear electrode (b)). The overall shape matches closely with the IPCE plot in **Fig. 9b**. The main difference is the relatively lower profile of the rear electrode in **Fig. S9b**. This is due to the absence of a rear reflector in the theoretical calculation, which decreases the light absorbed by the rear electrode in comparison with the experimental case in **Fig. 9b**.

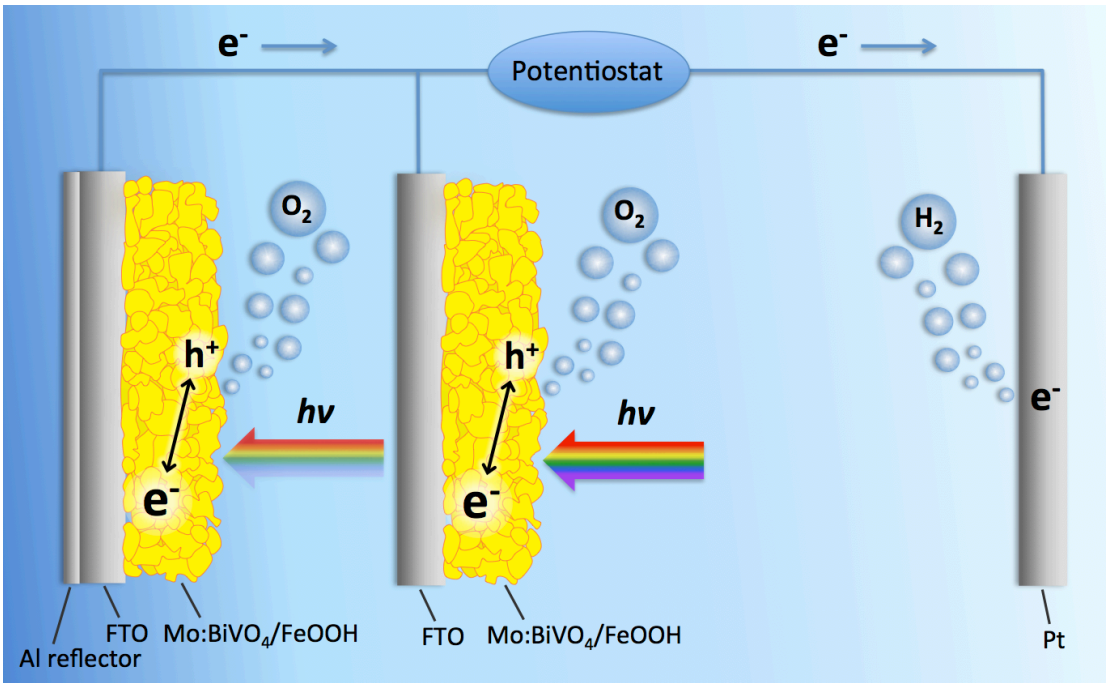

Fig. S12 Schematic representation of the double stacked Mo:$BiVO_4$/FeOOH electrode geometry. The reference electrode was omitted for clarity.

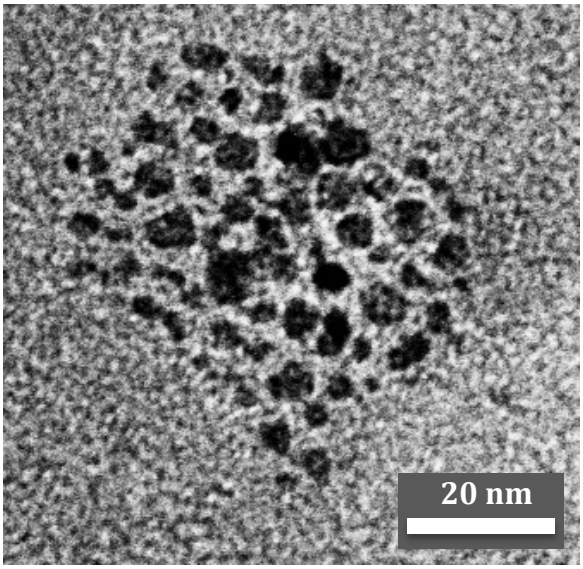

Fig. S13 TEM image of $NiFe_2O_4$ nanocrystals.

References

1. K. Sayama, A. Nomura, T. Arai, T. Sugita, R. Abe, M. Yanagida, T. Oi, Y. Iwasaki, Y. Abe and H. Sugihara, *J Phys Chem B*, 2006, **110**, 11352-11360.
2. S. P. Berglund, A. J. E. Rettie, S. Hoang and C. B. Mullins, *Phys Chem Chem Phys*, 2012, **14**, 7065-7075.
3. S. K. Pilli, T. E. Furtak, L. D. Brown, T. G. Deutsch, J. A. Turner and A. M. Herring, *Energ Environ Sci*, 2011, **4**, 5028-5034.
4. L. Trotochaud, J. K. Ranney, K. N. Williams and S. W. Boettcher, *J Am Chem Soc*, 2012, **134**, 17253-17261.
5. D. C. Hong, Y. Yamada, T. Nagatomi, Y. Takai and S. Fukuzumi, *J Am Chem Soc*, 2012, **134**, 19572-19575.
6. J. Rockenberger, E. C. Scher and A. P. Alivisatos, *J Am Chem Soc*, 1999, **121**, 11595-11596.
7. Z. F. Chen and T. J. Meyer, *Angew Chem Int Edit*, 2013, **52**, 700-703.
8. K. Sayama, N. N. Wang, Y. Miseki, H. Kusama, N. Onozawa-Komatsuzaki and H. Sugihara, *Chem Lett*, 2010, **39**, 17-19.